

Characterization of Superconducting Rings Using an in-field Hall Probe Magnetic Mapping System

X. Granados, S. Sena, E. Bartolomé, A. Palau, T Puig, X Obradors, M. Carrera, J. Amorós, H. Claus

Abstract—A Hall probe magnetic imaging system that works in magnetic fields in the range -1 T to 1 T has been implemented, and it has been used to characterize the superconducting behavior of single domain melt textured $\text{YBa}_2\text{Cu}_3\text{O}_7$ rings. We show that in addition to the analysis of the evolution of the local magnetic field distribution when the external magnetic field is cycled, the hysteretic behavior of the magnetic moment can also be investigated after integration of the local magnetic field. The critical current density has been determined through the critical state model and it has been compared to that calculated by inversion of the Biot-Savart law. A remarkable agreement is achieved with both methods.

Index Terms—Melt textured superconductors, Hall probes, Critical currents

I. INTRODUCTION

THE development of non-destructive and fast testing systems to evaluate the quality of superconducting materials remains a general objective in the field of applied superconductivity. Depending on the properties to be considered and the shape and size of the samples, several procedures have been proposed. In the field of bulk materials for motor and levitation applications, the levitation force and remanent flux profiles are being largely used. However, such tests are not suitable to compare material performances, because it is difficult to determine normalized superconducting parameters such as the critical current density.

The imaging of the remanent magnetisation by Hall probes is considered, by now, the most powerful test. This procedure not only gives global information of the sample but also allows to obtain information which correlates with the

distribution of defects on the sample. Recently, it has been shown that artificial joins of bulk melt textured $\text{YBa}_2\text{Cu}_3\text{O}_7$ (YBCO) can be obtained [1-3]. This novel technique has opened new avenues for practical applications where complex shapes are needed. The performance of these joints needs to be evaluated and the use of welded rings appear to be a very promising technique because the critical current of the weld can be evaluated with a very low voltage criterion through the induction of persistent currents when external magnetic fields are applied and no electrical contacts are needed [3]. The understanding of the electromagnetic behavior of ring-shaped superconducting materials appears then as a prerequisite.

A considerable effort has been devoted to obtain the current distribution in superconducting materials from magnetic flux profiles by solving the inverse problem [4]. In this way the local distribution of the critical current density can be imaged, thus, allowing to investigate the complex behavior of inhomogeneous or topologically connected materials such as rings.

At low fields, magneto-optical imaging is a powerful technique because external fields are easily applied. Hall probe magnetic imaging has also been demonstrated to be a powerful technique, giving direct measurements of the magnetic field, which can be extended to higher external magnetic fields [5]; however, it appears difficult to set up a scanning system under an external magnetic field.

In this work we report the use of an in-field Hall probe magnetic imaging system devised to work in applied fields in the -1 T to 1 T field range at 77 K. We investigate the field dependence of the magnetic behavior of a ring-shaped single domain melt textured YBCO sample, and we calculate the critical current density both from the magnetic flux distribution (solving the inverse problem) and from the magnetic moment using the critical state model.

II. EXPERIMENTAL

Single domain melt textured $\text{YBa}_2\text{Cu}_3\text{O}_7$ pellets were grown by Top Seeding Growth following processes previously described [1],[3],[6]. A ring shaped sample of YBCO has been obtained by drilling a thin disc. The size of the sample is $2R_{\text{ext}}=4.95$ mm of external diameter by $2R_{\text{int}}=3.15$ mm of inner diameter. The thickness of the sample is $t=0.53$ mm. The sample has been magnetically characterized

Manuscript received August 6, 2002. This work was supported in part by the European Commission under Grant RTN1-1999-00282, "Supermachines", the Spanish Science Ministry (MAT99-0855), by the Generalitat de Catalunya (00206) and Spain-USA cooperation program (2000-20195).

X. Granados, S. Sena, E. Bartolomé, A. Palau, T. Puig, X. Obradors are with the Institut de Ciència de Materials de Barcelona, Campus UAB, 08193 Bellaterra, Spain, (phone 34-93-580-18-53, fax 34-93-580-57-29, e-mail: granados@icmab.es).

M. Carrera is with Dept. Medi Ambient i Ciències del Sòl, Universitat de Lleida, Lleida, Spain. J. Amorós is with Dept. Matemàtica Aplicada, Universitat Politècnica de Catalunya, Barcelona, Spain

H. Claus is with the Material Science Division of the Argonne National Laboratory, USA

by measuring the magnetization cycle by means of a SQUID magnetometer. Hall measurements have been done with an GaAs Hall probe with an active area of $0.1 \times 0.1 \text{ mm}^2$. The probe is rastered, maintaining its active area at a flying distance of $\approx 80\text{-}100 \text{ }\mu\text{m}$, through the polished surface of the ring in steps of $160 \text{ }\mu\text{m}$. As shown in Fig. 1, the Hall raster has been designed to be operated in the gap of an electromagnet allowing magnetic imaging in applied field conditions. The Hall probe measures the local magnetic field $B(x,y)$ which has a contribution from the external magnetic field and also from the perpendicular component of the magnetic field generated by the induced currents flowing in the superconductor. The external magnetic field is applied perpendicular to the surface of the sample and the full hysteresis loop can be measured. The current distribution generating the observed magnetic flux profiles has been computed by solving the inverse problem with the software package Caragol [7]. This software package solves the Biot-Savart law for 3-D bulk samples assuming a planar current circulation, i.e. $J_z=0$, but without any assumption on the geometry of the planar current within the samples. Details about the mathematical procedure followed to compute an overdetermined linear equation system have been presented elsewhere [7]. A critical parameter is the height at which the magnetic image was measured with the Hall probe system, which needs to be well known for the calculation. We have tested the consistency of the inversion method from our magnetic imaging system by computing the current distribution from images taken at different heights in standardized samples [7]. In the present case the measurements were carried out at $100 \text{ }\mu\text{m}$. The comparison between the original measurements and the computed magnetic fields calculated with the current distribution gives differences lower than 5% which is established as coincidence criteria.

III. RESULTS AND DISCUSSION

Persistent currents flowing in the superconducting ring were induced either by applying external magnetic fields after Zero Field Cooling (ZFC) or Field Cooling (FC) processes.

The magnetic moment $\vec{m} = \frac{1}{2} \int \vec{r} \otimes \vec{J}(\vec{r}) d^3r$ of a type-II

superconductor induced by these currents can be calculated through the critical state model which assumes that $J(\mathbf{r})$ can not exceed the critical current J_c . We also assume that the reversible magnetization associated with the Meissner currents can be neglected, i.e., H_{c1} is much smaller than the magnetic fields considered in our experiments. We have investigated the flux distribution $B(x,y)$ as a function of the magnetic field by means of Hall probe magnetic imaging to verify that the induced magnetic moment has indeed the expected cylindrical symmetry. Fig. 2 reports a typical magnetic field profile $B(x,y)$ - H measured under magnetic field after a ZFC process, while Fig. 3 displays several typical $B(x)$ - H cross-sectional patterns measured when the magnetic field is first increased

up to $H= 2.3 \text{ kOe}$ and then reduced to zero. As it may be observed in Fig. 2, a perfect cylindrical symmetry is observed,

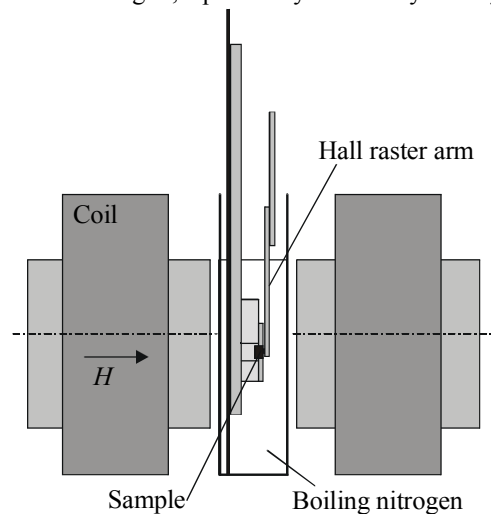


Fig. 1. Schematics of the in-field Hall probe magnetization mapping system.

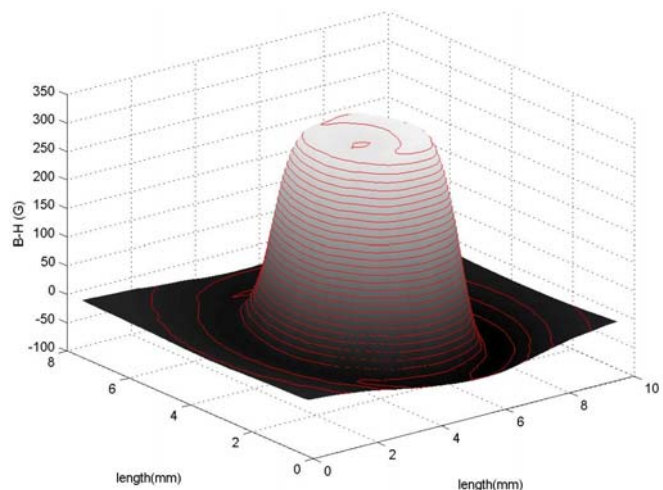


Fig. 2. Magnetic field distribution above a superconducting ring with an applied magnetic field of $H=400 \text{ Oe}$.

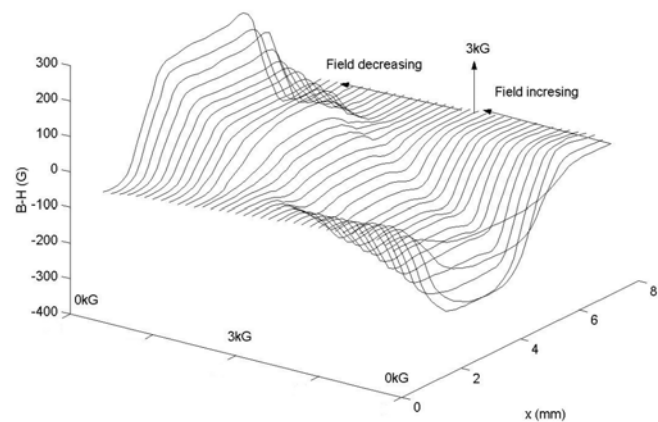


Fig. 3. Magnetic field profiles across the superconducting ring under different external magnetic fields after a Zero Field Cooling process.

thus confirming the good quality of the melt textured single domain YBCO ring used in the present work. Further details of the flux penetration process can be obtained by examining the field dependence of the magnetic flux profiles (Fig. 3). We can observe first an increase of the magnetic moment with a flat flux profile in the center of the ring while the induced current is increasing. At higher fields, the flat flux profile is preserved, but the magnetic moment decreases smoothly, thus indicating a decrease of the induced currents. Finally, we also observed that the homogeneity of the flux distribution is preserved during the reversal of the magnetic moment, which is a further proof of the quality of the sample.

The maximum current which may be induced in a ring with uniform current density across its thickness is

$$I_c = 2\pi t \int_{R_{int}}^{R_{ext}} J(r) dr.$$

This current is induced when the field penetration H_p is achieved. If we assume that the critical current density is field independent, the magnetic moment at

$$H > H_p \text{ is } m(H) = \frac{\pi}{3} J_c t (R_{ext}^3 - R_{int}^3)$$

and then the magnetic moment should remain field independent [8]. Usually, however, the critical currents in melt textured YBCO are field dependent [9] and also demagnetizing effects inducing inhomogeneous current density $J(r)$ can occur [8], depending on the dimensions of the ring, so the applicability of these theoretical predictions should be tested in real materials.

For this purpose we have in addition measured the isothermal magnetization by means of a SQUID magnetometer, and we have compared the hysteresis loop with the mean local "magnetization" over the whole ring surface defined as $\bar{B} - H = \frac{1}{4\pi R_{ext}^2} \iint [B_z(x, y) - H] dx dy$. Fig. 4

displays both magnitudes as a function of the magnetic field. We can see that a perfect coincidence among both magnitudes is achieved when $\bar{B} - H$ is multiplied by a field independent constant $k \approx 1.95$. We should note also that the observed magnetic remanence at zero field equals that observed after a FC process, thus indicating that the maximum external magnetic field was higher than $2H_p$. The coincidence of the field dependence of both hysteretic magnetizations will allow us to calculate directly the field dependence of the critical current density $J_c(H)$ from the local magnetic flux measured with the in-field Hall probe magnetic imaging system. An additional feature which should be noted is that in the low field limit the isothermal magnetization has a linear behavior, a characteristic which has been found to be very useful in the investigation of welded rings [3]. At low magnetic fields the ring can be modeled, in a first approximation, as a single-turn solenoid. The field dependence of the magnetic moment can be calculated taking into account that the magnetic flux inside the ring remains null $m(H) = I \cdot S$, $S \approx \pi R_{ext}^2$, $I \approx (\mu_0 \pi R_{ext}^2 / L) \cdot H$ where L is the self-inductance of a ring

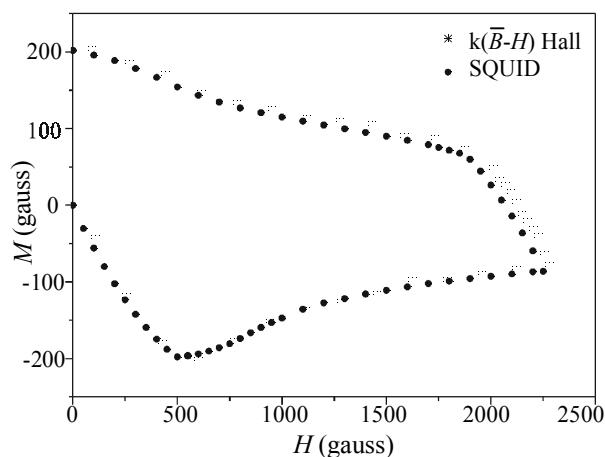


Fig. 4. Magnetization hysteresis loops measured with the SQUID magnetometer and the mean magnetization $\bar{B} - H$ measured with the Hall microprobes.

$$L = \mu_0 \left(\frac{R_{ext} + R_{int}}{2} \right) \left[\ln 8 \left(\frac{R_{ext} + R_{int}}{R_{ext} - R_{int}} \right) - 2 \right] \quad [10] \text{ and hence } m(H) \approx$$

$(\mu_0 \pi^2 R_{ext}^4 / L) \cdot H$, i.e. a linear behavior is found. At high fields, however, the non-linear terms associated with the critical state flux penetration model become relevant and so the virgin magnetization curve becomes non-linear [8], as observed in Fig. 4. Because of this non-linear behavior and the field dependence of the critical current density $J_c(H)$, the penetration field H_p may not coincide with the observed magnetization peak (Fig. 4) [8]. We have verified, however, that the slope of the magnetic moment at the origin in the virgin $m(H)$ curve (Fig. 4) agrees with the expected geometrical value for a single-turn solenoid. We note also that the same slope is found when the sign of the magnetic field sweep is reversed at high magnetic field (Fig. 4). This is because the flux crossing the inner ring surface is preserved while the induced currents in the ring are changing sign, and so the same self-inductance determines the change of the magnetic moment.

Now, we can calculate the critical current density J_c of the ring on one side using the critical state model and the measured magnetic moment $m(H)$, and on the other side, we can carry out a deconvolution of the magnetic flux distribution using the Biot-Savart law

$$B_z(r) = \frac{\mu_0}{4\pi} \iiint \frac{\vec{J}(r') \otimes (\vec{r} - \vec{r}')}{(r - r')^3} d^3 r'.$$

The critical state model adapted to ring-shaped samples with $R_{ext} \gg t$, and $R_{int} \gg t$ [8]

$$\text{states that } J_c(H) = \frac{3}{\pi t} \left(\frac{1}{R_{ext}^3 - R_{int}^3} \right) m(H).$$

Fig. 5 shows the results of this calculation for the melt textured ring investigated in the present paper. We note that the calculated critical current density at zero field, i.e., $J_c(0) \approx 2.8 \cdot 10^4 \text{ A/cm}^2$, and the observed field dependence are typical of bulk single domain YBCO samples at 77 K [6],[9].

The calculation of the local current density $J_c(x, y)$ from the observed magnetic field distribution $B(x, y)$ was performed

using the software package Caragol [7]. Fig. 6 (a) displays the computed current distribution superposed on the measured magnetic field distribution after a FC process while Fig. 6 (b) displays a particular cross section of this current distribution. We can observe that the homogeneity of the current density is preserved and also that the limits where the current vanishes are close to the external surfaces of the ring. The peak values of the critical current density at zero field computed by this method are $J_c(0) \approx 1.5 \cdot 10^4$ A/cm², while at $H=2.2$ kOe $J_c(H) \approx 4 \cdot 10^3$ A/cm², values which appear to be in rather good agreement with those calculated from the critical state model (Fig. 5), thus validating the consistency of our imaging system.

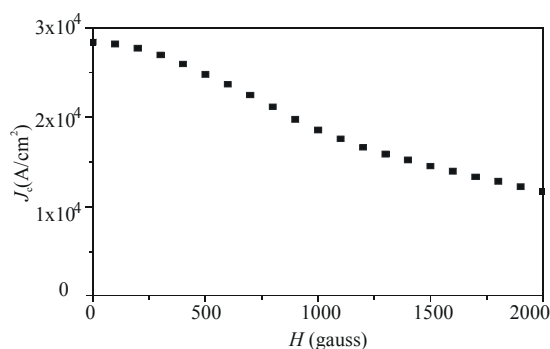


Fig. 5. Field dependence of the critical current calculated by means of the critical state model from the magnetic moment measured with a SQUID magnetometer.

IV. CONCLUSIONS

We have validated an in-field Hall probe magnetic imaging system by measuring the field dependence of the magnetic moment of a single domain melt textured YBCO ring. The magnetic field profiles are characteristic of an homogeneous material and the integrated local magnetic field follows the same magnetic field dependence than the whole magnetic moment thus allowing to use the critical state model to calculate the critical current density. The induced currents have been calculated as well by solving the Biot-Savart law.

ACKNOWLEDGMENT

This work is dedicated to Prof. Domingo González from University of Zaragoza and ICMA-CSIC on the occasion of his retirement.

REFERENCES

[1] H. Zheng, H. Claus, L. Chen, A. P. Paulikas, B. W. Veal, B. Olsson, A. Koshelev, J. Hull, G. W. Crabtree, G. A. Boyd, "Transport currents measured in ring samples: test of superconductor weld," *Physica C*, vol. 350, pp. 17-24, 2001.

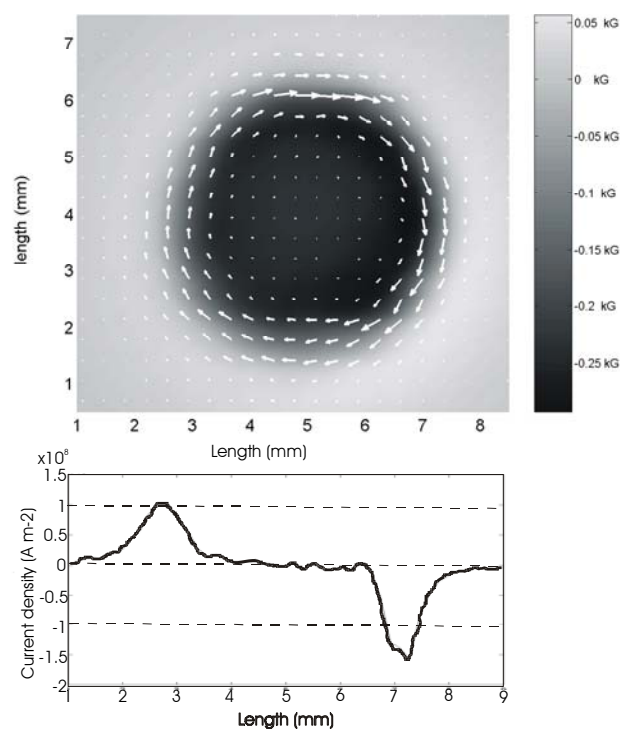


Fig. 6. Current distribution as calculated by solving the inverse problem with the magnetic flux distribution in the remanent state by means of the Biot-Savart law.

- [2] T. Puig, P. Rodrigues Jr., A. E. Carrillo, X. Obradors, H. Zheng, U. Welp, L. Chen, H. Claus, B. W. Veal, G. W. Crabtree, "Self-seeded YBCO welding induced by Ag additives," *Physica C*, vol. 363, pp. 75-79, 2001.
- [3] H. Claus, U. Welp, H. Zheng, L. Chen, A. P. Paulikas, B. W. Veal, K. E. Gray and G. W. Crabtree, "Critical current across grain boundaries in melt textured YBa₂Cu₃O_{7-δ} rings," *Phys.Rev.B*, vol. 64, pp. 144507, 2001.
- [4] Ch. Joos, J. Albrecht, H. Kuhn, S. Leonhardt and H. Kronmüller, "Magneto-optical studies of current distributions in high-T_c superconductors," *Rep.Prog.Phys.*, vol. 65, pp. 651-788, 2002.
- [5] G. K. Perkins, Y. Bugoslavsky, X. Qi, J. L. MacManus-Driscoll, A. D. Caplin, "High field scanning Hall probe imaging of high temperature superconductors," *IEEE Trans.Appl.Supercond*, vol. 11, pp. 3186-3189, 2001.
- [6] X. Obradors , R. Yu , F. Sandiumenge , B. Martinez , N. Vilalta , V. Gomis , T. Puig , S. Piñol, "Directional solidification of ReBa₂Cu₃O₇ (Re=Y,Nd) : microstructure and superconducting properties," *Supercond. Sci. Technol*, vol. 10, pp. 884-890, 1997.
- [7] J. Amorós, M. Carrera, X. Granados, J. Fontcuberta, X. Obradors, "Computation of critical current through magnetic flux profile measurements," in *Applied Superconductivity 1997*, Inst. of Phys. Conf. Series No. 158, pp. 1639-1642, 1998.
- [8] E. H. Brandt, "Susceptibility of superconductor discs and rings with and without flux creep," *Phys.Rev.B*, vol. 55, pp. 14513-14526, 1997.
- [9] B. Martínez , V. Gomis, A. Gou, S. Piñol, J. Fontcuberta, X. Obradors, H. van Tol, "Critical currents and pinning mechanisms in directionally solidified YBa₂Cu₃O₇-Y₂BaCuO₅ composites," *Phys.Rev.B*, vol. 53 , pp. 2797- 2810, 1996.
- [10] L. D. Landau and E. M. Lifshitz, "Electrodynamics of Continuous Media," Oxford: Pergamon, 1963, Chap.6.